repl. c.

NACA

RESEARCH MEMORANDUM

EFFECT OF DIHEDRAL CHANGE ON THE THEORETICAL DYNAMIC LATERAL RESPONSE CHARACTERISTICS OF A LOW-ASPECT-RATIO STRAIGHT-WING SUPERSONIC AIRPLANE

By Donovan R. Heinle

Ames Aeronautical Laboratory
Moffett Field, Calif.

NATIONAL ADVISORY COMMITTEE
FOR AERONAUTICS

WASHINGTON
December 7, 1950

NATIONAL ADVISORY COMMITTEE FOR AERONAUTICS

RESEARCH MEMORANDUM

EFFECT OF DIHEDRAL CHANGE ON THE THEORETICAL DYNAMIC LATERAL RESPONSE CHARACTERISTICS OF A LOW-ASPECT-RATIO STRAIGHT-WING SUPERSONIC AIRPLANE

By Donovan R. Heinle

SUMMARY

Results of a theoretical investigation of the lateral response and stability characteristics of the X-3 research airplane (Douglas Model No. 499D, Study 41-B) are presented. Included are time histories calculated by the Reeves Electronic Analog Computer showing the effect of various disturbances on the lateral response of the airplane with 0° geometric dihedral (normal configuration) and with -5° dihedral. Two sets of values of the yawing moment due to roll were used, one estimated using present theory and the other based on recent wind-tunnel tests of an X-3 model.

The calculations show that the airplane is oscillatorily and spirally stable with either dihedral but does not meet the U. S. Air Force period-damping requirements in any high-speed condition investigated. The rolling motions and the roll excitation parameter $\left(\left|\frac{\varphi}{\beta}\right|\right)$ are generally large for the airplane with 0° dihedral; these rolling motions are reduced considerably by a change to -5° dihedral. The nature of the motions following application of a step rolling moment appear normal with either dihedral. The initial roll (and the eventual roll, with -5° dihedral at high speeds) following an abrupt step rudder deflection is in an adverse direction; however, these unusual rolling motions are small compared to those which can be produced by the ailerons. The only significant effect produced by a change in the yawing moment due to roll parameter from the estimated value to a more negative value based on experimental results is a marked reduction in the damping of the oscillatory mode.

INTRODUCTION

A general study of the predicted motions of various high-speed aircraft configurations is being made at the Ames Aeronautical Laboratory. The influence of design trends on the flying qualities of airplanes is of interest. It is believed that examination of the predicted motions, in the light of results of flight studies such as those reported in reference 1 and the specifications as given in reference 2, will indicate both the characteristics of the motion of high-speed configurations which may be undesirable and the design changes necessary to improve the behavior.

One example of these high-speed configurations is the X-3 airplane (fig. 1) which makes use of a comparatively low-aspect-ratio straight wing. This airplane might be considered representative of a future design trend which will resort to low-aspect-ratio wings with supersonic wing sections to minimize high-speed drag. This trend is in contrast to another making use of swept wings.

Previous theoretical studies on the dynamic lateral stability characteristics of an early version of the X-3 airplane (reference 3) and on a later modification of the X-3 (reference 4) indicated, in addition to deficiencies in oscillatory period-damping relations, large excitation of rolling motions due to yawing disturbances. Recent flight tests of a conventional fighter airplane equipped with a device for varying effective wing dihedral in flight (reference 1) have shown that this roll excitation is an important item in the handling characteristics. In view of these results and the fact that the X-3 configuration had been altered considerably since the study of reference 3, it was considered desirable to make additional dynamic lateral-stability studies with the latest available wind-tunnel and dimensional data and to study the effect of a possible change to negative dihedral on the flying qualities. The study of the rolling motions due to yawing disturbances also was of interest.

During this investigation reference 5 was published dealing with the period-damping relationship as affected by a change to -5° geometric dihedral and variations in some of the dynamic stability derivatives. It also included a short discussion of the $\left|\frac{\varphi}{\beta}\right|$ relationship applied to one flight condition.

This report includes a more detailed discussion and data on the $\left|\frac{\varphi}{\beta}\right|$ relationship over the operating Mach number range of the X-3 airplane for 0° and -5° geometric dihedral. Several time histories of step and pulse disturbances are included showing the typical lateral motions of the airplane.

SYMBOLS

The data presented herein are referred to the stability system of axes. The positive directions of the forces, moments, and angular displacements are shown in figure 2. The stability system of axes is defined as an orthogonal system having its origin at the center of gravity and in which the Z axis is in the plane of symmetry and perpendicular to the relative wind, the X axis is in the plane of symmetry and perpendicular to the Z axis, and the Y axis is perpendicular to the plane of symmetry.

φ	angle of bank measured about the X axis, radians
ψ	angle of yaw measured about the Z axis, radians
β	angle of sideslip $\left(\frac{v}{V}\text{, where } v \text{ is the lateral velocity in the Y direction}\right)$, radians
p	rolling velocity measured about the X axis, radians per second
r	yawing velocity measured about the Z axis, radians per second
V	true airspeed, feet per second
ρ	mass density of air, slugs per cubic foot
q	dynamic pressure $\left(\frac{1}{2}\rho V^2\right)$, pounds per square foot
b	wing span, feet
S	wing area, square feet
W	weight of airplane, pounds
m	mass of airplane, slugs
μ	relative density factor $\left(\frac{m}{\rho S b}\right)$
Γ	geometric dihedral, degrees
η	inclination of principal longitudinal axis of airplane with respect to flight path, positive when principal axis is above flight path at nose, degrees
α	angle between reference axis and flight path, positive when reference axis is above flight path at the nose, degrees
γ	angle of flight path to horizontal axis, positive in climb, degrees

k_{x_o} radius of gyration in roll about principal longitudinal axis, feet

k_{z_o} radius of gyration in yaw about principal vertical axis, feet

K_{x_o} nondimensional radius of gyration in roll about principal longitudinal axis $\left(\frac{k_{x_o}}{b}\right)$

K_{z_o} nondimensional radius of gyration in yaw about principal vertical axis $\left(\frac{k_{z_o}}{b}\right)$

K_x nondimensional radius of gyration in roll about longitudinal stability axis $\left(\sqrt{{K_{x_o}}^2 \cos^2\eta + {K_{z_o}}^2 \sin^2\eta}\right)$

K_z nondimensional radius of gyration in yaw about vertical stability axis $\left(\sqrt{{K_{z_o}}^2 \cos^2\eta + {K_{x_o}}^2 \sin^2\eta}\right)$

K_{xz} nondimensional product-of-inertia parameter

$$\left[\left({K_{z_o}}^2 - {K_{x_o}}^2\right) \sin \eta \cos \eta\right]$$

C_L lift coefficient

C_l rolling-moment coefficient $\left(\frac{\text{rolling moment}}{qSb}\right)$

C_n yawing-moment coefficient $\left(\frac{\text{yawing moment}}{qSb}\right)$

C_Y lateral-force coefficient $\left(\frac{\text{lateral force}}{qS}\right)$

$C_{n_{\delta_r}}$ yawing-moment coefficient due to rudder deflection, per degree

$C_{l_{\delta_r}}$ rolling-moment coefficient due to rudder deflection, per degree

t time, seconds

D differential operator $\left(\frac{d}{dt}\right)$

P period of oscillation, seconds

$T_{\frac{1}{2}}$ time for amplitude of oscillation to decrease by one-half

M Mach number

Subscripts

β rate of change with angle of sideslip $\left(\frac{\partial}{\partial\beta}\right)$

p rate of change with rolling-angular-velocity factor $\left[\frac{\partial}{\partial\,(pb/2V)}\right]$

r rate of change with yawing-angular-velocity factor $\left[\frac{\partial}{\partial(rb/2V)}\right]$

A applied disturbance

est estimated

rev revised

COMPUTATION METHODS

The responses to simple roll and yaw disturbances were determined for eight flight conditions for both the normal configuration with 0° geometric dihedral and for one with -5° geometric dihedral. These flight conditions listed in table I covered the expected operating ranges of Mach number from 0.30 to 2.0 and altitude from sea level to 50,000 feet.

Time Histories

The time histories of the motion of the airplane were calculated from the equations of motion in the following form:

$$\left(2\mu\ K_X{}^2D^2 - \frac{1}{2}\frac{V}{b}C_{l_p}\ D\right)\varphi + \left(2\mu\ K_{XZ}D^2 - \frac{1}{2}\frac{V}{b}C_{l_r}\ D\right)\psi -$$

$$\left(\frac{V}{b}\right)^2 C_{l_\beta}\ \beta = C_{l_A}\left(\frac{V}{b}\right)^2$$

$$\left(2\mu\ K_{XZ}\ D^2 - \frac{1}{2}\frac{V}{b}C_{n_p}\ D\right)\varphi + \left(2\mu\ {K_Z}^2 D^2 - \frac{1}{2}\frac{V}{b}C_{n_r}\ D\right)\psi -$$

$$\left(\frac{V}{b}\right)^2\ C_{n_\beta}\ \beta = C_{n_A}\ \left(\frac{V}{b}\right)^2$$

$$\left(-\frac{1}{2}C_{Y_p}D - \frac{V}{b}C_L\right)\varphi + \left[\left(2\mu - \frac{1}{2}C_{Y_r}\right)D - \frac{V}{b}C_L\tan\gamma\right]\psi +$$

$$\left(2\mu\ D - \frac{V}{b}C_{Y_\beta}\right)\beta = C_{Y_A}\left(\frac{V}{b}\right)$$

For all conditions the flight path was assumed to be level ($\gamma = 0$) and both C_{Y_p} and C_{Y_r} were assumed to be zero.

The Reeves Electronic Analog Computer (REAC) was employed to plot directly as a function of time the lateral response of the airplane as specified by the equations given above. In these plots it was desirable to maintain as large an amplitude of the output of the REAC as possible for a given case so that the period-damping relationship could be measured with the greatest possible accuracy. The time histories presented herein are photographic reductions of these direct plots made at various scale values and care must be used in comparing the curves. Time histories of the responses φ, ψ, β, and their derivatives for the following inputs are computed by the REAC for each case:

1. Rectangular yawing-moment pulse,

   $C_n = 0.01$ for 0.15 second

2. Step rolling moment, $C_l = 0.01$
3. Step yawing moment, $C_n = 0.01$

In addition to these three inputs, time histories of the motion due to a step rudder deflection and due to an initial sideslip were obtained for a few conditions.

Lateral Characteristics

For each condition, P, $T_{\frac{1}{2}}$, and $\left|\frac{\varphi}{\beta}\right|$ were obtained by calculating directly by the usual means from the complex roots of the characteristic equation, and by scaling these values directly from time histories obtained by use of the REAC. The method given in the appendix was used to calculate the ratio of the amplitude of the oscillatory mode of angle of bank φ to sideslip angle β (written $\left|\frac{\varphi}{\beta}\right|$ and tentatively chosen as a measure of roll excitation, reference 1).

Airplane Characteristics

The stability derivatives and dimensions for the airplane, presented in table I, were obtained from references 4 and 6 supplemented by additional information from the Douglas Aircraft Company.

The values of C_{n_p}, used originally in the present investigation, were estimated in the usual manner (reference 4) and were used in the original calculations and REAC studies. It was found in tests of a model similar in configuration to the X-3 in the stability tunnel at the Langley Aeronautical Laboratory that these values of C_{n_p} were in error (reference 5). Consequently, revised values of C_{n_p} were calculated from the following formula based on the experimental data:

$$C_{n_{p_{rev}}} = C_{n_{p_{est}}} - \left(0.125 \frac{C_{Y_{\beta_{tail}}}}{-0.30}\right)$$

The lateral characteristics were recalculated with $C_{n_{p_{rev}}}$ for all test conditions, and REAC studies were repeated for those conditions considered of greatest interest (I, II, and VII).

RESULTS AND DISCUSSION

Although time histories of the airplane motion were obtained and analyzed for all the conditions listed, only those representative of high lift coefficient at sea level (I), high subsonic speed at sea level (II), and supersonic flight at moderately high altitude (VII) have been included herein. The motions for these widely differing conditions are indicative of the nature of the motions for the other conditions. The revised values of C_{n_p} were used for all the time histories which are presented except where noted on the figures.

Representative plots for each of the inputs listed under the section Time Histories are included. The pulse input furnishes a good representation of the oscillatory mode of response as also does the initial sideslip input. The latter also provides an indication of gust response of the airplane. The two step inputs provide a method for separating the effect of rolling and yawing-moment components due to ailerons or rudder on the response. The step rudder deflection provides one example of an arbitrary control deflection for the study of the nature of the resulting motion.

Response to a Pulse Yawing Moment

The time histories of the lateral response of the airplane to a yawing-moment pulse are presented in figure 3 for 0° and -5° geometric dihedral. As may be seen from the figure, this type of input serves to excite primarily the oscillatory mode of motion. Direct examination indicates that, although there is little change in the nature and magnitude of the motions in ψ or β as a result of the change in dihedral, the relatively large roll with 0° dihedral is considerably reduced by -5° dihedral, particularly at high speeds. The small initial negative roll in condition I arises due to the fact that the yawing moment is applied about an axis different from the principal axis. This fact makes the term K_{XZ} large enough so that the yawing acceleration produces a noticeable disturbance in the rolling-moment equation. The same effect will be noted later in the response to a rudder deflection.

Response to a Step Rolling Moment

For this airplane, the motions due to an applied step rolling moment (fig. 4) represent closely those in a rudder-fixed aileron roll, since the yawing moment due to aileron deflection is small. The nature of the motions appears to be normal. Fairly large adverse sideslip and a resulting reduction in rolling velocity are indicated for condition I; the initial sideslip and yawing motions arise primarily from product-of-inertia effects at this high angle of attack. It has been ascertained on magnified plots that at high speeds the sideslip is negligible, the yaw is small compared to the roll, and the rolling velocity reaches the maximum rapidly and remains essentially constant after 1 second.

Response to a Step Yawing Moment

The response to a step yawing moment with a dihedral of 0° (fig. 5) reflects the same characteristics as the response to the pulse yawing moment (fig. 3). A small negative initial roll occurs in condition I, and the rolling motions in the other conditions are large compared to the yawing motions. Data not presented in this report show that a change to -5° dihedral reduced the rolling amplitude.

For given control-effectiveness parameters, time histories of the response to arbitrary control deflections can be approximated by suitable superposition of the step-response data of figures 4 and 5.

Response to a Step Rudder Deflection

The lateral response due to 1° step rudder deflection for the airplane with either 0° or -5° dihedral (fig. 6) shows an initial adverse roll. In the high-speed conditions, this is due primarily to the large rolling moment contributed by the rudder. In the low-speed condition I, however, the initial adverse roll arises primarily from the large positive inclination of the principal axis; this effect was noted previously in connection with airplane motions due to a yawing-moment pulse. With a dihedral of 0°, the effective dihedral is sufficiently positive to overcome the initial rolling tendencies and to cause rolling in the normal direction after 1 second or so. At high speeds with dihedral equal to -5° (figs. 6(b) and 6(c)), the effective dihedral is not sufficiently positive to overcome the rolling moment due to rudder deflection, and the airplane starts and continues to roll in the adverse direction.

It is probable that a pilot would be conscious of the small initial erratic rolling motions primarily as an unusually long delay in the development of normal rolling motion. Since the adverse roll during the first second or two is small, little use of the rudder appears necessary at high speeds in view of the very small sideslip angles which would occur in aileron-roll maneuvers.

Response to an Initial Sideslip

The time histories of the motion due to an initial sideslip (fig. 7) are indicative of the action of the airplane in gusty air; the response can be considered as that due to a sharp-edged side gust of velocity $v = V\beta$. With a dihedral of 0°, the nature of the motion appears normal except for the low damping of the oscillatory mode and the rather high excitation of the rolling motion, especially at high speed. The sizable reduction in rolling amplitudes at high speeds due to a change in dihedral to -5° is apparent; the sideslip and yawing motions are almost the same between the two values of dihedral.

Lateral Oscillation Characteristics

It can be demonstrated that any type of input resulting in control-fixed oscillations will produce the same values of the period P, time to damp to half amplitude $T_{\frac{1}{2}}$, and the parameter $\left|\frac{\varphi}{\beta}\right|$. Since the yawing-moment pulse input produces a well-defined lateral oscillation (fig. 3, for example), these time histories were used to obtain most of the REAC values of P, $T_{\frac{1}{2}}$, and $\left|\frac{\varphi}{\beta}\right|$. The values of P, $T_{\frac{1}{2}}$, and $\left|\frac{\varphi}{\beta}\right|$ as scaled from the REAC data and as calculated directly are given in table II for the various combinations of C_{n_p} and dihedral.

The calculated values of $T_{\frac{1}{2}}$ are plotted as a function of P in figure 8, along with the period-damping criterion boundary of reference 2. The change in dihedral from 0° to −5° with $C_{n_{p_{rev}}}$ (fig. 8(a)) shows a favorable effect with regard to position relative to the boundary for all but condition VIII, where damping was decreased slightly. Sizable increases in damping are apparent in conditions II, III, and VII.

With regard to $\left|\frac{\varphi}{\beta}\right|$, examination of table II will show that the change to −5° dihedral produced a reduction in the roll excitation. For a dihedral equal to 0°, $\left|\frac{\varphi}{\beta}\right|$ ranged from 3.34 to 5.59. The change to −5° reduced $\left|\frac{\varphi}{\beta}\right|$ to 3.30 or less for all conditions. The results reported in reference 1 indicate that lateral oscillations characterized by slightly unsatisfactory period-damping relations and values of $\left|\frac{\varphi}{\beta}\right|$ greater than about 4.0 may be intolerable. In order to safeguard against this possibility with this airplane, use of a negative dihedral angle or a means of improving the period-damping characteristics would be needed. Unfortunately, use of −5° dihedral might lead to a reversal of lateral stick position and control force in steady sideslips because of the large rolling moments due to rudder deflections.

The change from $C_{n_{p_{est}}}$ to $C_{n_{p_{rev}}}$ was found to have little effect on the response characteristics except for a decrease in the damping of the oscillatory mode. This is readily apparent in comparing figure 8(a) with 8(b). More of the conditions (fig. 8) are in the unsatisfactory range with $C_{n_{p_{rev}}}$ mainly because of the changes in time to damp to half amplitude. The dihedral change was found to be more effective with $C_{n_{p_{rev}}}$ than with $C_{n_{p_{est}}}$.

It was found that the values of P, $T_{\frac{1}{2}}$, and $\left|\frac{\varphi}{\beta}\right|$ obtained from the time histories as computed by use of the REAC agree with these values as calculated directly from the characteristic equations within ±5 percent for P and within ±10 percent for $T_{\frac{1}{2}}$ and $\left|\frac{\varphi}{\beta}\right|$.

CONCLUSIONS

The following conclusions may be drawn from the present analysis of the lateral response characteristics of a high-speed straight-wing airplane configuration with 0° (normal) and −5° geometric wing dihedral: (Unless otherwise noted, values of the stability derivative C_{n_p} are based on recent wind-tunnel data.)

1. The airplane is oscillatorily and spirally stable with 0° dihedral, but does not meet the Air Force period-damping requirements (reference 2) in any high-speed condition investigated. A change in dihedral to −5° generally results in an increase in damping or in period (both favorable), but unsatisfactory period-damping relationships are still indicated.

2. For the airplane with dihedral equal to 0°, the rolling motions following a yawing disturbance are large, and the ratio of the amplitudes of the oscillatory mode of angle of bank to angle of sideslip $\left|\frac{\varphi}{\beta}\right|$ ranges from 3.34 to 5.59. These values, coupled with the damping deficiencies noted above, indicate an airplane which would be slightly tolerable to intolerable as measured by pilot evaluation. With dihedral equal to −5°, these rolling motions are considerably reduced and the roll excitation parameter $\left(\left|\frac{\varphi}{\beta}\right|\right)$ is less than 3.30 for all con- conditions – indicating a tolerable or better airplane.

3. The initial roll following an abrupt step rudder deflection is in an adverse direction; that is, right roll follows a left rudder deflection. With dihedral equal to 0°, the dihedral effect is sufficient to cause rolling in the normal direction after 1 second or so. With dihedral equal to −5°, the roll continues in the adverse direction at high speeds. For either dihedral these rolling motions are small compared to those which can be produced by the ailerons. The adverse roll, therefore, may not be a serious deficiency in view of the small rudder deflections required to maneuver the airplane at high speeds.

4. The nature of the motions following application of a step rolling moment appears normal for the airplane with either 0° or −5° dihedral. At high speeds, the sideslip is very small and the rolling velocity reaches a maximum rapidly and remains essentially constant after 1 second.

5. The only significant effect of a change in the values of the yawing moment due to roll parameter (C_{n_p}) from those estimated in the usual manner to the more negative values based on recent wind-tunnel data was a marked reduction in damping of the oscillatory mode.

Ames Aeronautical Laboratory,
National Advisory Committee for Aeronautics,
Moffett Field, Calif.

APPENDIX

CALCULATION OF THE ROLL EXCITATION PARAMETER $\left(\left|\frac{\varphi}{\beta}\right|\right)$

As indicated in the appendix of reference 7, the oscillatory mode of the response in bank φ of an airplane to an applied unit step yawing disturbance may be written as a function of time:

$$(I + Ji)_{\varphi_N} e^{\lambda_3 t} + (I - Ji)_{\varphi_N} e^{\lambda_4 t} \qquad (1)$$

and the oscillatory mode of the response in sideslip β as

$$(I + Ji)_{\beta_N} e^{\lambda_3 t} + (I - Ji)_{\beta_N} e^{\lambda_4 t} \qquad (2)$$

where

$$\left.\begin{array}{l} \lambda_3 = a + bi \\ \lambda_4 = a - bi \end{array}\right\} \text{complex roots of the characteristic stability equation}$$

$$\left.\begin{array}{l} (I + Ji)_{\varphi_N} \\ (I - Ji)_{\varphi_N} \\ (I + Ji)_{\beta_N} \\ (I - Ji)_{\beta_N} \end{array}\right\} \text{complex response coefficients}$$

Expressions (1) and (2) may be rewritten:

$$2(I_{\varphi_N} + J_{\varphi_N} i)\ e^{at} \cos b(t + t_{\varphi_N}) \qquad (3)$$

$$2(I_{\beta_N} + J_{\beta_N} i)\ e^{at} \cos b(t + t_{\beta_N}) \qquad (4)$$

where the time intervals t_{φ_N} and t_{β_N} account for differences in phase.

The ratio of the amplitudes of the oscillatory modes of φ to β may be obtained by neglecting the periodic cosine functions and dividing equation (3) by equation (4). This yields:

$$\left|\frac{\varphi}{\beta}\right| = \left|\frac{I_{\varphi_N} + J_{\varphi_N} i}{I_{\beta_N} + J_{\beta_N} i}\right| \tag{5}$$

The terms I_{φ_N}, J_{φ_N}, I_{β_N}, and J_{β_N} are obtained by substitution of the root $\lambda_s = a + bi$ in the Heaviside expansion theorem. Thus,

$$\left|I_{\varphi_N} + J_{\varphi_N} i\right| = \left[\frac{|f(\lambda_s)|}{|\lambda_s F'(\lambda_s)|}\right]_{\varphi_N} \tag{6}$$

and

$$\left|I_{\beta_N} + J_{\beta_N} i\right| = \left[\frac{|f(\lambda_s)|}{|\lambda_s F'(\lambda_s)|}\right]_{\beta_N} \tag{7}$$

where f represents the appropriate minor determinant and F' the derivative of the major determinant. Since the denominators of equations (6) and (7) are identical, equation (5) may be written:

$$\left|\frac{\varphi}{\beta}\right| = \frac{|f(\lambda_s)|\varphi_N}{|f(\lambda_s)|\beta_N} \tag{8}$$

The expression $|f(\lambda_s)|_{\varphi_N}$ is evaluated by expanding the determinant obtained by replacing the φ column in the equations of motion by the column 0, 1, 0 and substituting λ_s. Similar operation on the β column yields $|f(\lambda_s)|_{\beta_N}$. For the equations of motion used in the present investigation, the following expression results:

$$\left|\frac{\varphi}{\beta}\right| = \left| \frac{\left[-\left(\frac{V}{b}\right)^2 C_{l_\beta}\right]\left[\left(2\mu - \frac{1}{2}C_{Y_r}\right)D - \frac{V}{b}C_L \tan\gamma\right] - \left(2\mu D - \frac{V}{b}C_{Y_\beta}\right)\left(2\mu K_{XZ}D^2 - \frac{1}{2}\frac{V}{b}C_{l_r}D\right)}{\left(-\frac{1}{2}C_{Y_p}D - \frac{V}{b}C_L\right)\left(2\mu K_{XZ}D^2 - \frac{1}{2}\frac{V}{b}C_{l_r}D\right) - \left[\left(2\mu - \frac{1}{2}C_{Y_r}\right)D - \frac{V}{b}C_L \tan\gamma\right]\left(2\mu K_X{}^2 D^2 - \frac{1}{2}\frac{V}{b}C_{l_p}D\right)} \right| \tag{9}$$

where λ_s is substituted for D.

Examination and elimination of numerically insignificant terms from the above equation gave the following expression, accurate to within ±6 percent for the cases considered herein:

$$\left|\frac{\varphi}{\beta}\right| = 0.93 \left| \frac{\left[2\mu K_{XZ} b^{1} - \left(\frac{V}{b}\right)^2 C_{l_\beta}\right] + \left(-4\mu K_{XZ} a^{1} b^{1} + \frac{1}{2}\frac{V}{b}C_{l_r} b^{1}\right) i}{\left(2\mu K_X{}^2 b^{1}\right) + \left(-4\mu K_X{}^2 a^{1} + \frac{1}{2}\frac{V}{b}C_{l_p}\right) i} \right| \tag{10}$$

where a^1 and b^1 are the real and imaginary parts, respectively, of λ_s.

REFERENCES

1. Liddell, Charles J., Jr., Van Dyke, Rudolph, D., Jr., and Heinle, Donovan R.: A Flight Determination of the Tolerable Range of Effective Dihedral on a Conventional Fighter Airplane. NACA TN 1936, 1949.

2. Anon.: Flying Qualities of Piloted Airplanes. U. S. Air Force Specification No. 1815-B, 1948.

3. Bennett, Charles V.: Theoretical Investigation of the Dynamic Lateral Stability Characteristics of Douglas Design No. 39C, An Early Version of the X-3 Research Airplane. NACA SRM L8L31, 1949.

4. Douglas Aircraft Company: Dynamic Lateral Stability of the MX-656 Airplane – 499D, Report No. SM-13429, Dec. 23, 1948.

5. Bennett, Charles V.: Theoretical Investigation of the Dynamic Lateral Stability Characteristics of the Douglas X-3 Research Airplane, Study 41-B. NACA SRM L50B28, 1950.

6. Douglas Aircraft Company: Estimated Stability and Control Characteristics, Model 499D, Report No. SM-13415, Nov. 26, 1948.

7. Harper, Charles W., and Jones, Arthur L.: A Comparison of the Lateral Motion Calculated for Tailless and Conventional Airplanes. NACA TN 1154, 1947.

TABLE I.– MASS AND AERODYNAMIC DATA OF THE AIRPLANE USED IN CALCULATION OF TIME HISTORIES

[W = 20,800 pounds; S = 166.52 square feet; b = 22.69 feet]

CONDITION	I	II	III	IV	V	VI	VII	VIII
M	0.30	0.85	1.10	0.60	0.85	1.10	2.00	2.00
Altitude	0	0	20,000	35,000	35,000	35,000	35,000	50,000
γ	0	0	0	0	0	0	0	0
C_L	.942	.117	.152	.997	.497	.297	.090	.184
μ	71.894	71.894	134.936	232.288	232.288	232.288	232.288	473.585
α	15.31	1.54	1.81	14.85	6.55	3.54	2.07	4.23
η	12.36	–1.41	–1.14	11.90	3.60	0.59	–0.88	1.28
K_x^2	.01981	.01158	.01154	.01924	.01219	.01149	.01151	.01154
K_z^2	.18519	.19342	.19346	.18576	.19281	.19351	.19349	.19344
K_{xz}	.03807	–.00448	–.00362	.03679	.01141	.00191	–.00280	.00407
C_{l_p}	–.268	–.371	–.428	–.288	–.313	–.403	–.297	–.286
C_{l_r}	.192	.216	.339	.225	.256	.328	.161	.147
C_{n_r}	–1.000	–1.075	–1.840	–1.045	–1.150	–1.933	–1.020	–1.070
$C_{n_{p_{est}}}$	–.042	.181	.356	–.046	.110	.357	.174	.174
$C_{n_{p_{rev}}}$	–.211	–.003	.040	–.225	–.090	.018	.020	.011
C_{y_β}	–.726	–.761	–1.078	–.750	–.800	–1.133	–.690	–.710
C_{n_β}	.28077	.31515	.66468	.30369	.35526	.72198	.26931	.29223
C_{l_β} (Γ=0°)	–.13179	–.12606	–.18336	–.13752	–.13752	–.17190	–.09741	–.08595
C_{l_β} (Γ=–5°)	–.08137	–.05931	–.10429	–.08137	–.07077	–.09283	–.05587	–.04441
$C_{Y_p}=C_{Y_r}$	0	0	0	0	0	0	0	0
$C_{n_{\delta_r}}$	–.00339	–.00388	–	–	–	–	–.00116	–
$C_{l_{\delta_r}}$	.00011	.00112	–	–	–	–	.00030	–

NACA

TABLE II.– LATERAL OSCILLATION CHARACTERISTICS OF THE AIRPLANE

Condition	$C_{n_{p_{rev}}}$											
	$\Gamma = 0^\circ$						$\Gamma = -5^\circ$					
	REAC			Calculated			REAC			Calculated		
	P	$T_{\frac{1}{2}}$	$\left\|\frac{\varphi}{\beta}\right\|$	P	$T_{\frac{1}{2}}$	$\left\|\frac{\varphi}{\beta}\right\|$	P	$T_{\frac{1}{2}}$	$\left\|\frac{\varphi}{\beta}\right\|$	P	$T_{\frac{1}{2}}$	$\left\|\frac{\varphi}{\beta}\right\|$
I	2.45	1.44	3.42	2.45	1.46	3.34	2.70	1.47	2.99	2.69	1.43	2.97
II	1.45	2.68	4.44	1.46	2.75	4.63	1.44	1.74	2.02	1.48	1.78	2.12
III	–	–	–	1.18	2.73	4.25	–	–	–	1.17	2.18	2.27
IV	–	–	–	2.40	2.97	3.36	–	–	–	2.67	3.04	2.96
V	–	–	–	2.29	3.67	4.96	–	–	–	2.46	3.75	3.30
VI	–	–	–	1.46	2.27	3.79	–	–	–	1.47	2.22	2.16
VII	1.40	3.70	5.38	1.38	3.59	5.59	1.38	2.81	3.01	1.36	2.87	3.05
VIII	–	–	–	1.75	3.75	4.64	–	–	–	1.79	4.02	2.66

Condition	$C_{n_{p_{est}}}$											
	$\Gamma = 0^\circ$						$\Gamma = -5^\circ$					
	REAC			Calculated			REAC			Calculated		
	P	$T_{\frac{1}{2}}$	$\left\|\frac{\varphi}{\beta}\right\|$	P	$T_{\frac{1}{2}}$	$\left\|\frac{\varphi}{\beta}\right\|$	P	$T_{\frac{1}{2}}$	$\left\|\frac{\varphi}{\beta}\right\|$	P	$T_{\frac{1}{2}}$	$\left\|\frac{\varphi}{\beta}\right\|$
I	2.40	1.28	3.38	2.46	1.31	3.35	2.77	1.40	2.93	2.74	1.38	3.00
II	1.55	1.52	5.28	1.55	1.50	5.18	1.50	1.45	2.20	1.48	1.47	2.14
III	1.22	1.11	4.42	1.18	1.05	4.30	1.19	1.24	2.28	1.15	1.18	2.21
IV	2.50	2.32	3.57	2.41	2.27	3.38	2.78	2.45	3.20	2.69	2.38	2.98
V	2.36	2.42	5.30	2.33	2.37	5.09	2.61	2.60	3.25	2.49	2.76	3.33
VI	1.53	1.50	4.13	1.48	1.48	3.91	1.54	1.76	2.32	1.49	1.73	2.20
VII	1.42	1.84	5.86	1.42	1.81	5.94	1.39	1.98	3.14	1.37	1.90	3.09
VIII	1.83	2.52	4.86	1.76	2.54	4.71	1.85	3.20	2.50	1.80	3.08	2.69

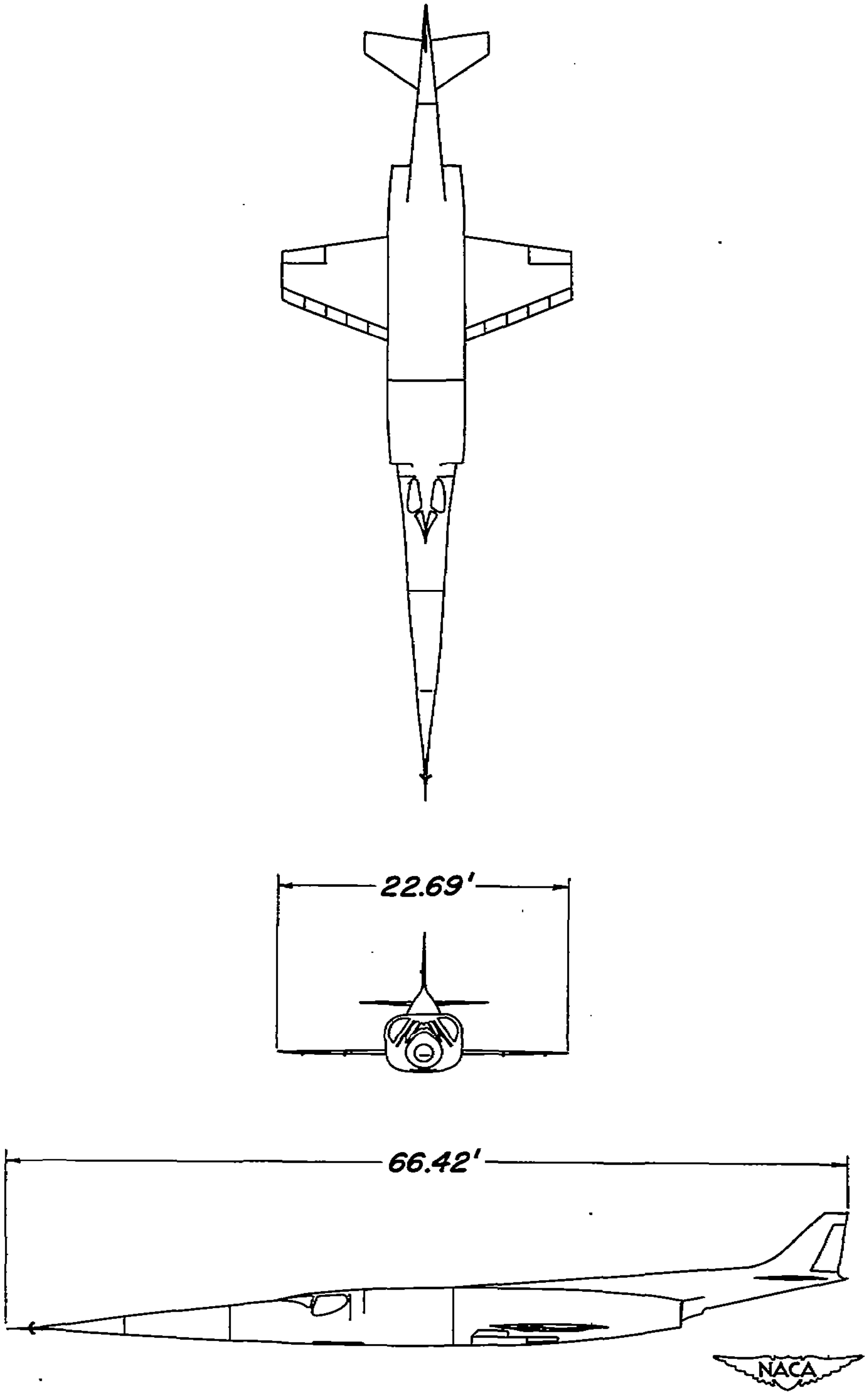

Figure 1.- Three-view sketch of the airplane.

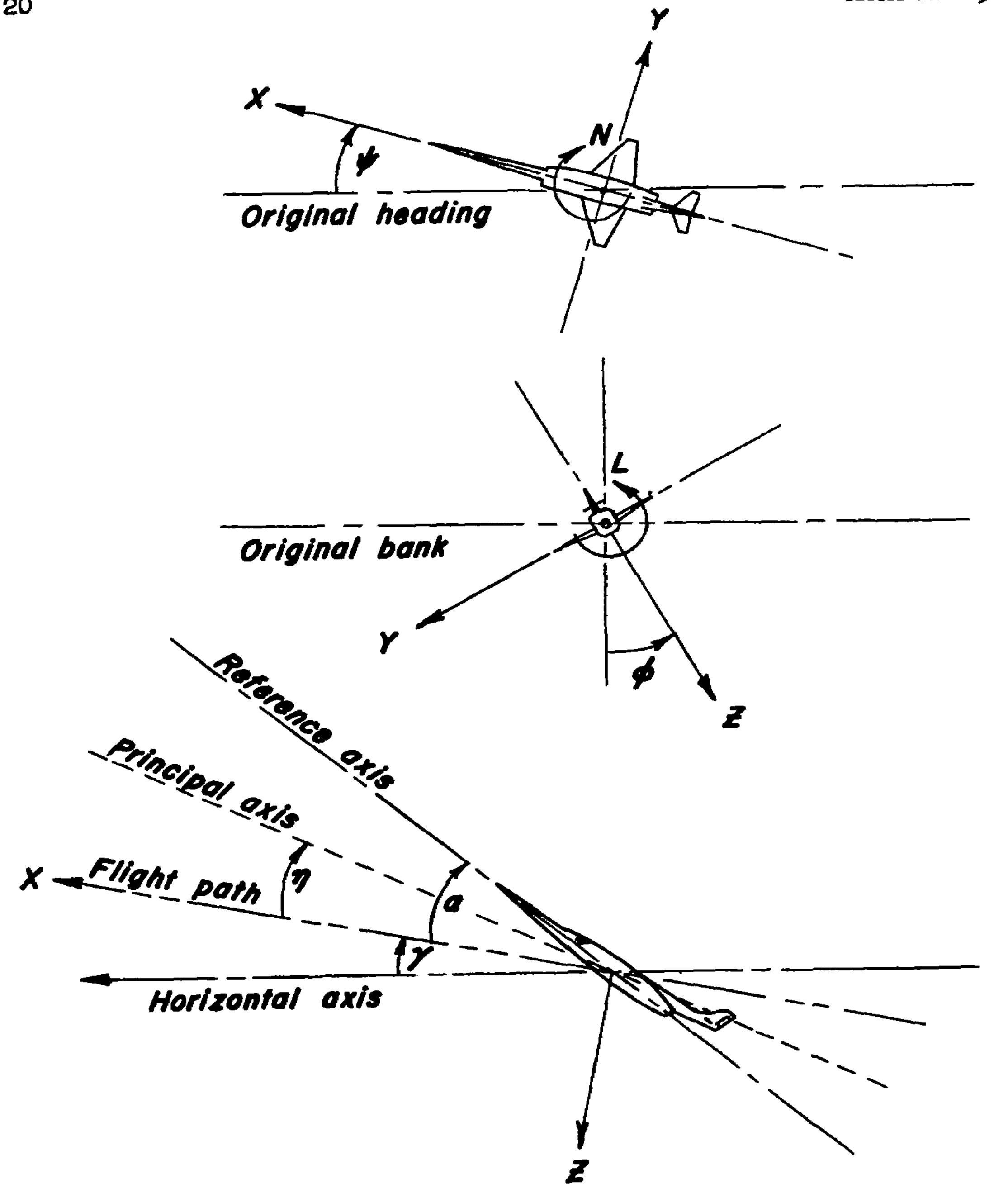

Figure 2.- Stability system of axes and angular relationships in flight. Arrows indicate positive direction of angles.

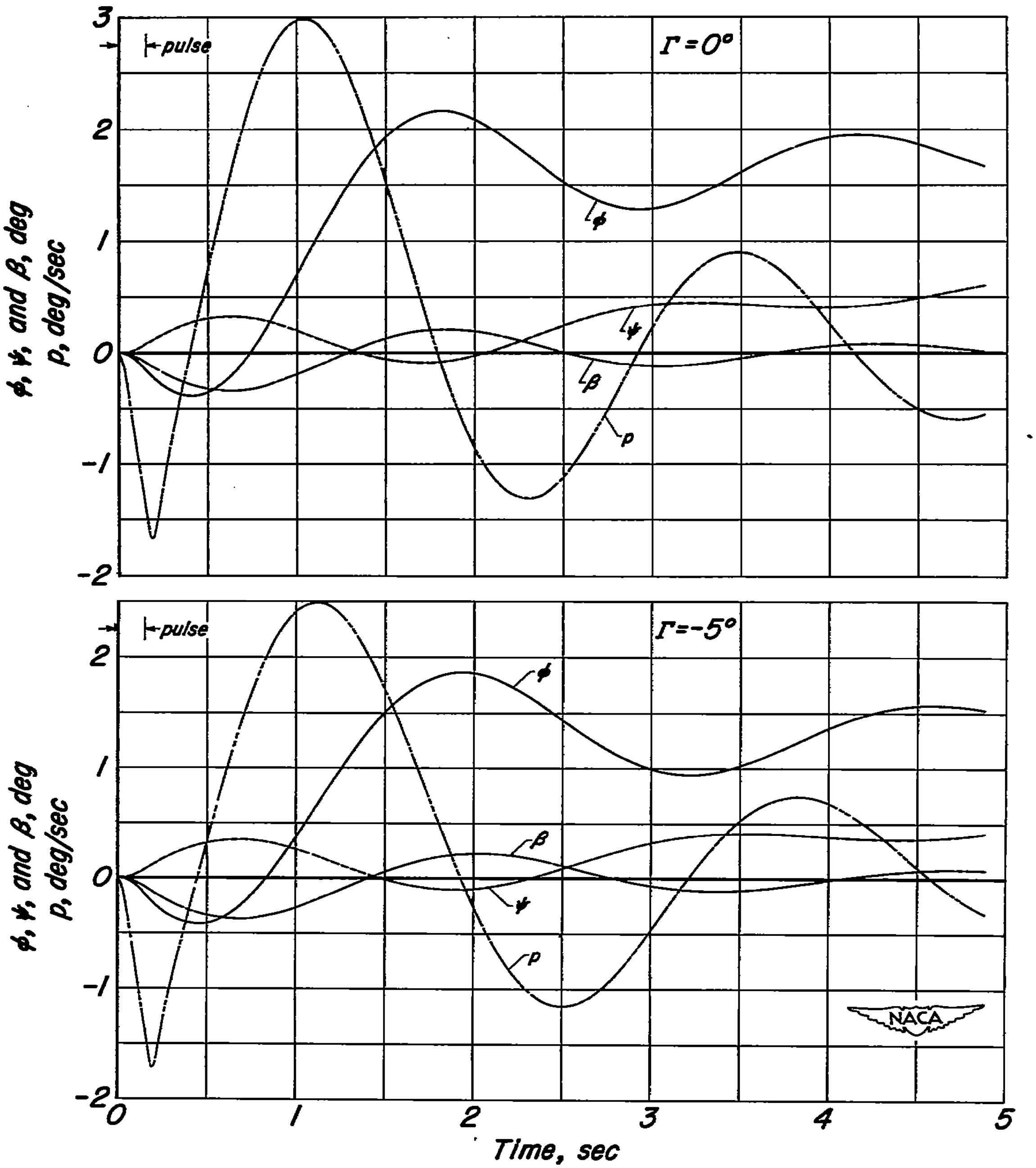

(a) Condition I, $M = 0.30$ at sea level.

Figure 3.- Lateral motion due to an applied yawing moment rectangular pulse.

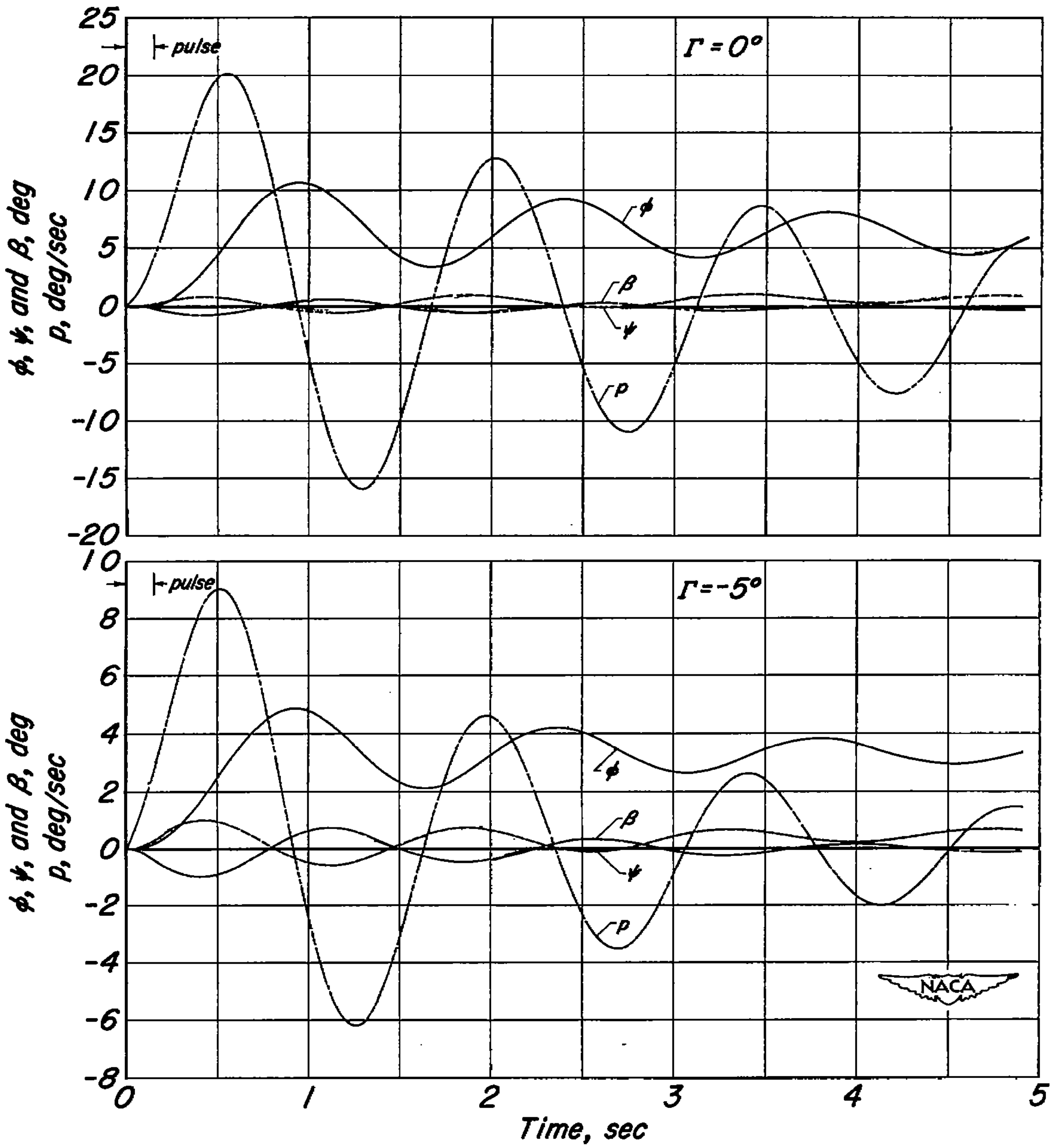

(b) Condition II, M = 0.85 at sea level.

Figure 3.- Continued.

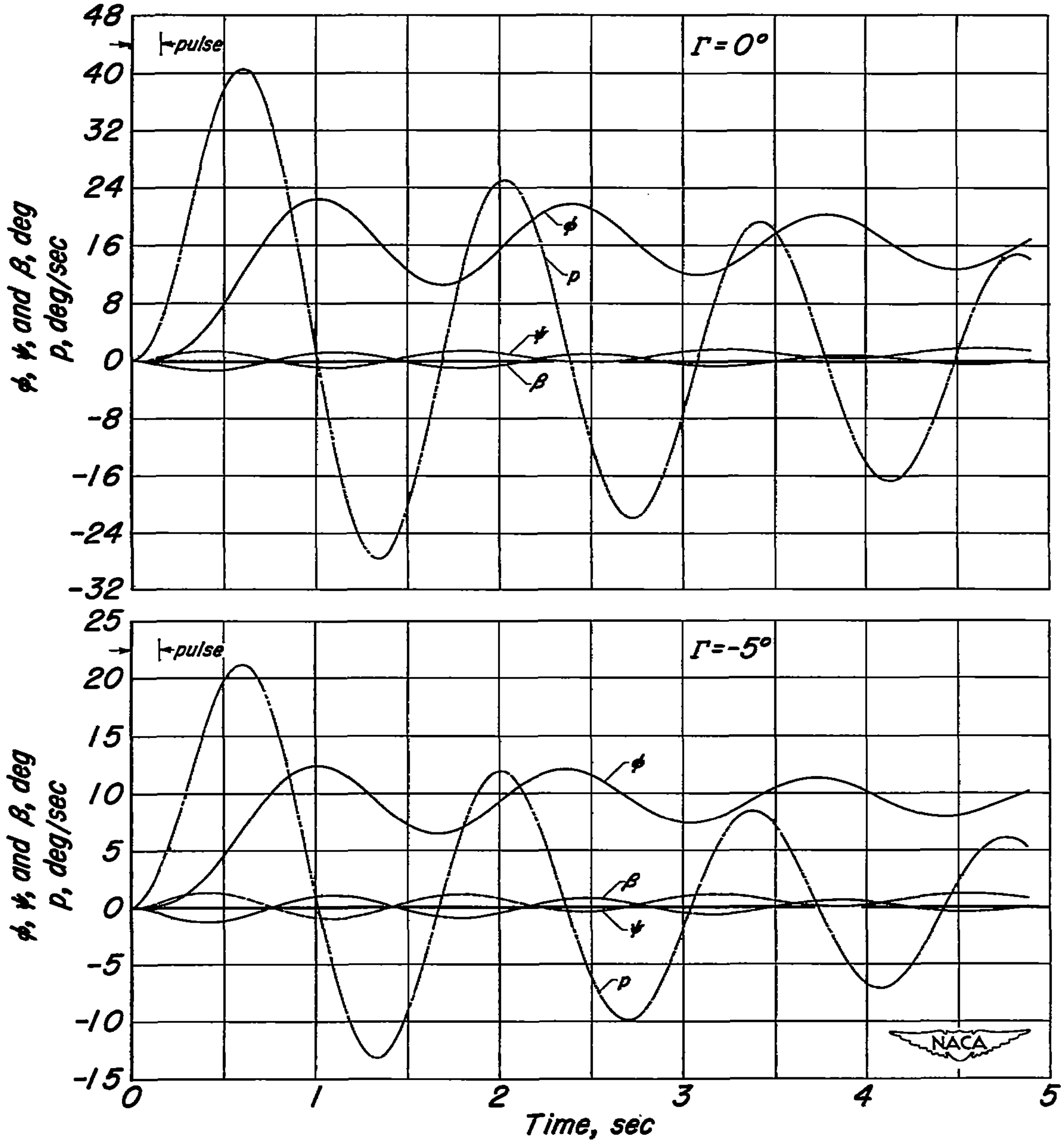

(c) Condition VII, M = 2.0 at 35,000 feet.

Figure 3.– Concluded.

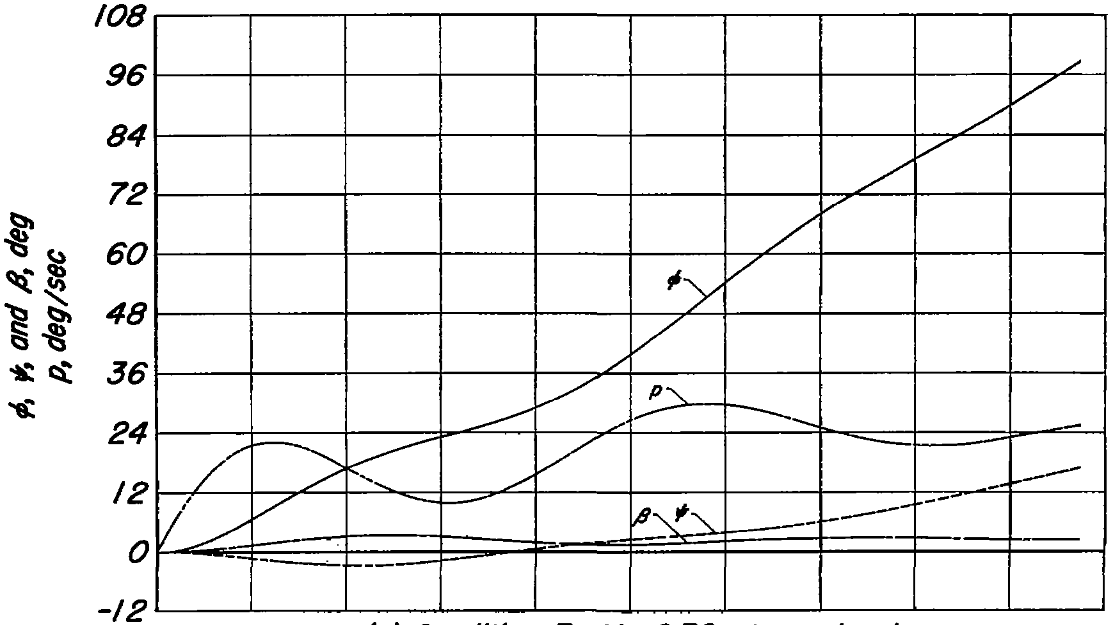

(a) Condition I, M = 0.30 at sea level.

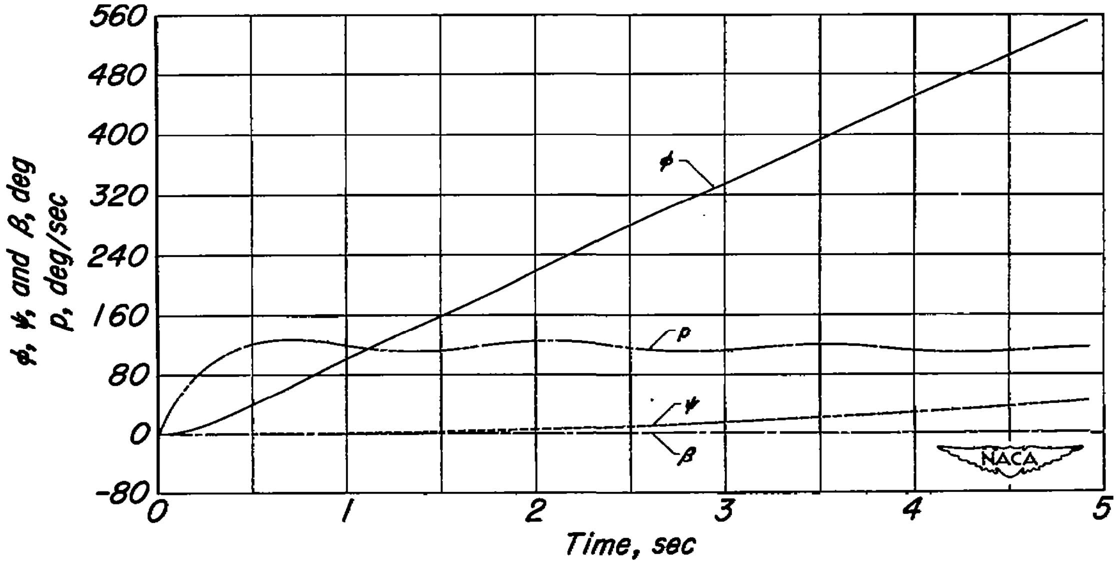

(b) Condition II, M = 0.85 at sea level.

Figure 4.- Lateral motion due to an applied step rolling moment; $\Gamma = 0°$.

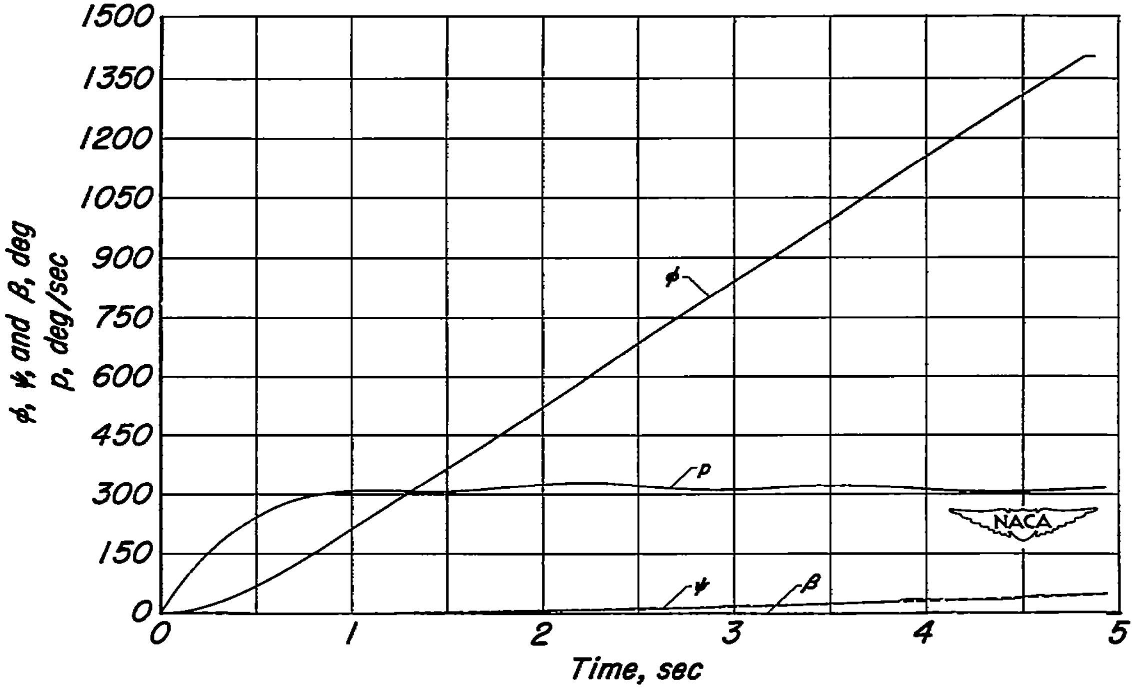

(c) Condition VII, M = 2.0 at 35,000 feet.

Figure 4.- Concluded.

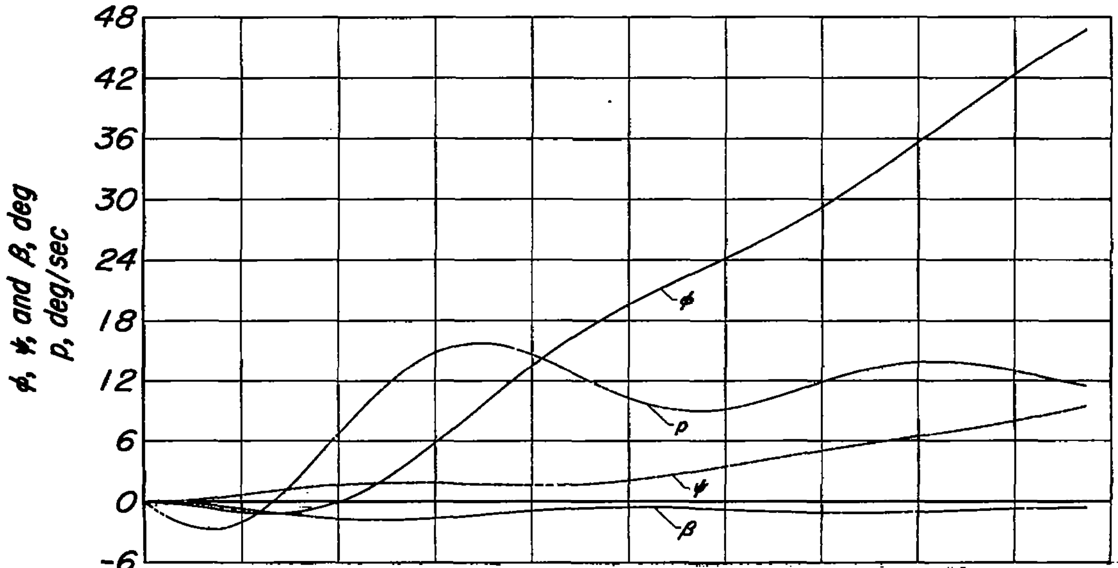

(a) Condition I, M = 0.30 at sea level.

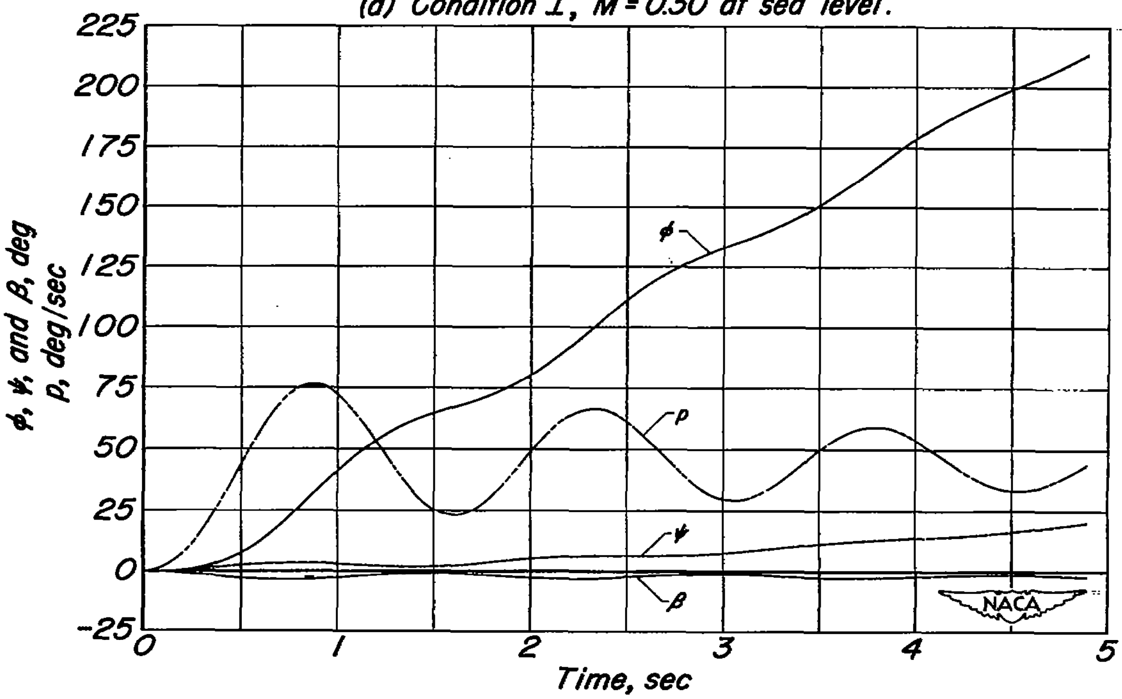

(b) Condition II, M = 0.85 at sea level.

Figure 5.- Lateral motion due to an applied step yawing moment; Γ = 0°.

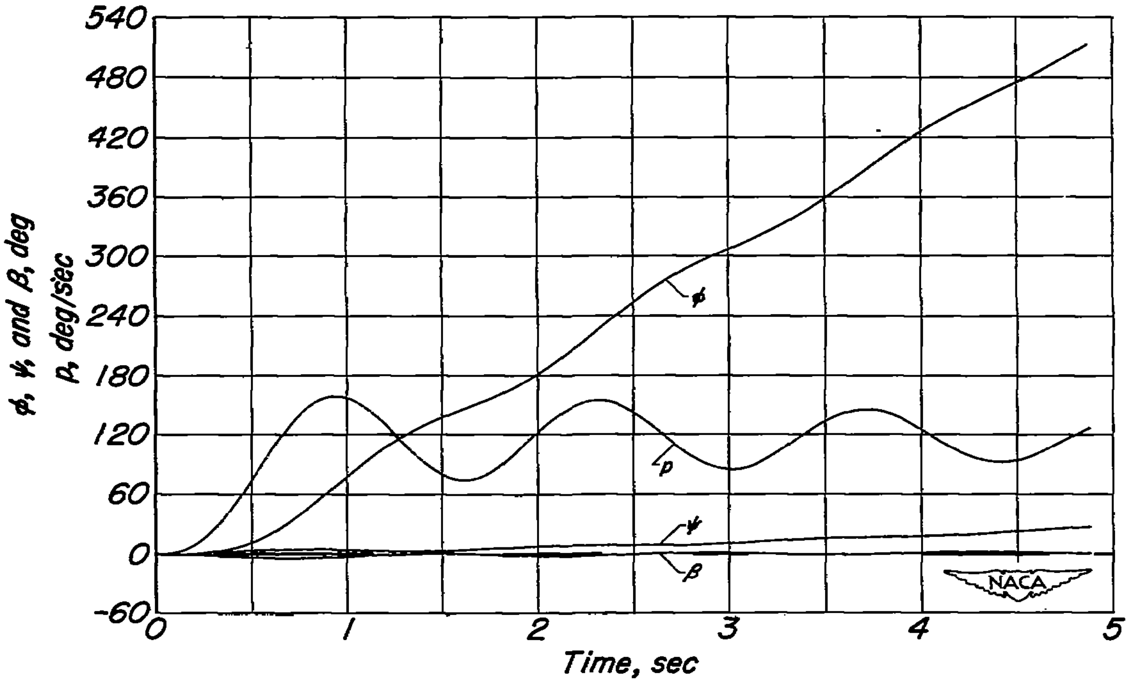

(c) Condition VII, M = 2.0 at 35,000 feet.

Figure 5.- Concluded.

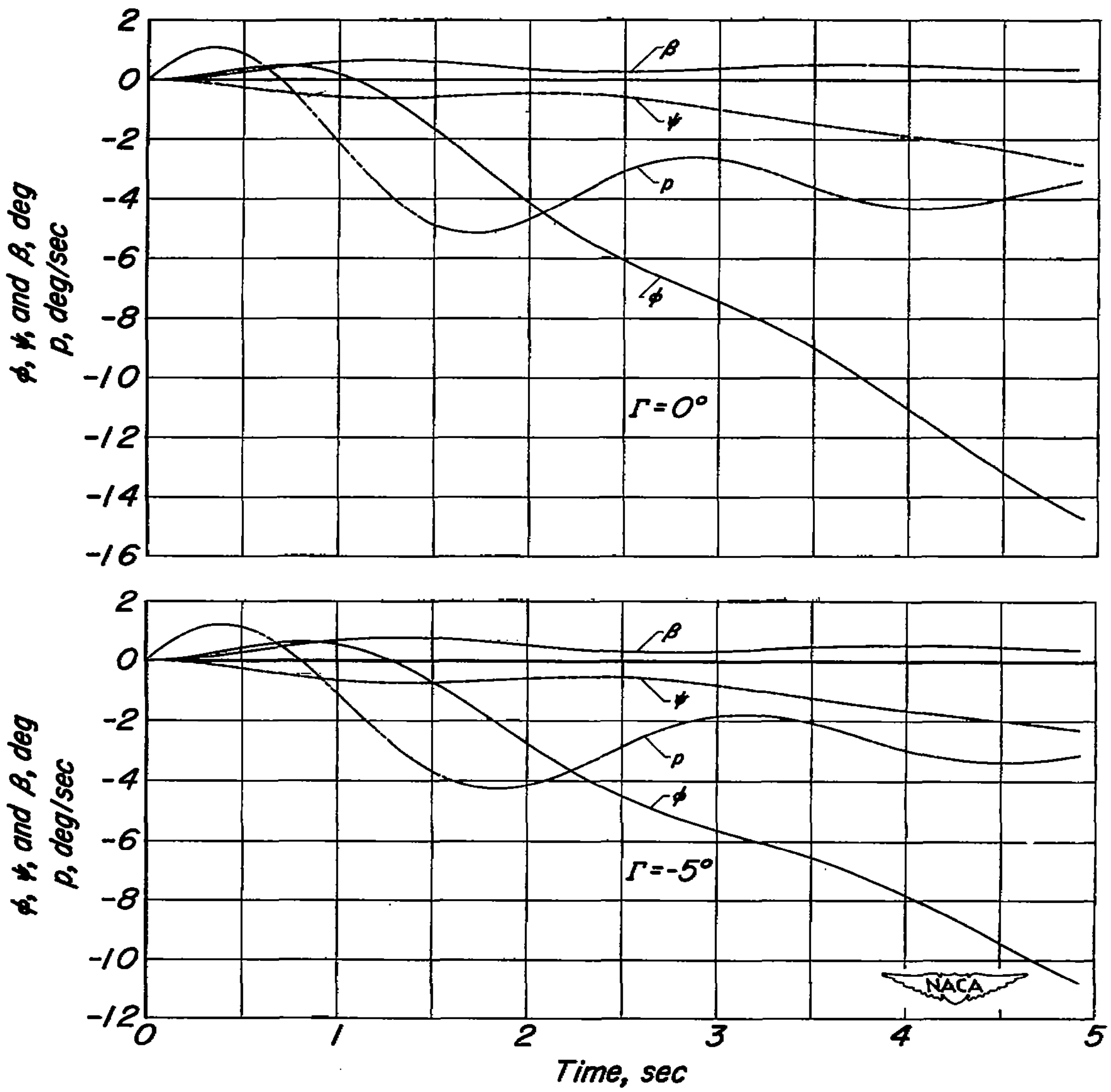

(a) Condition I, M = 0.30 at sea level.

Figure 6.- Lateral motion due to a 1° step left rudder deflection.

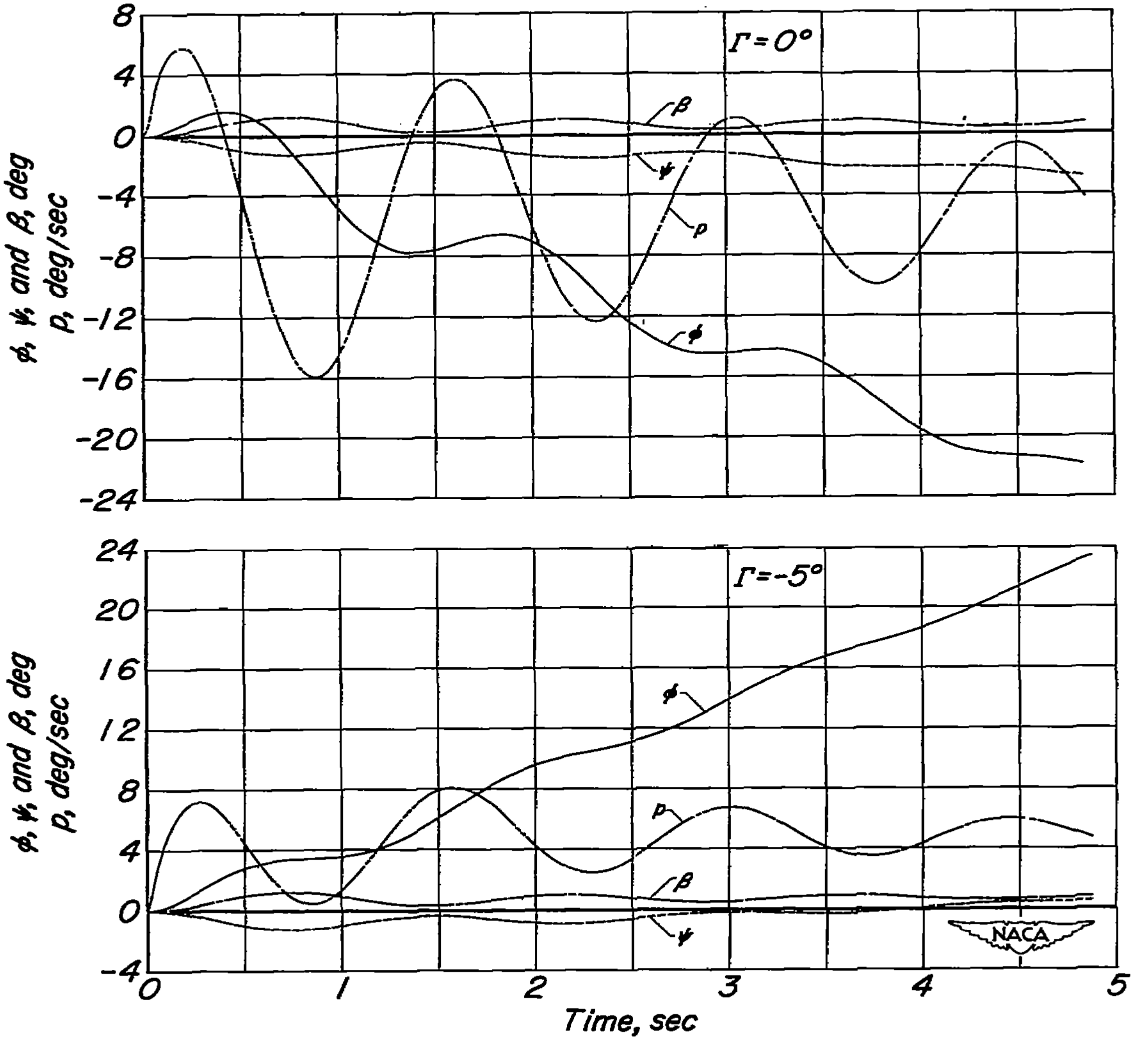

(b) Condition II, M = 0.85 at sea level.

Figure 6.- Continued.

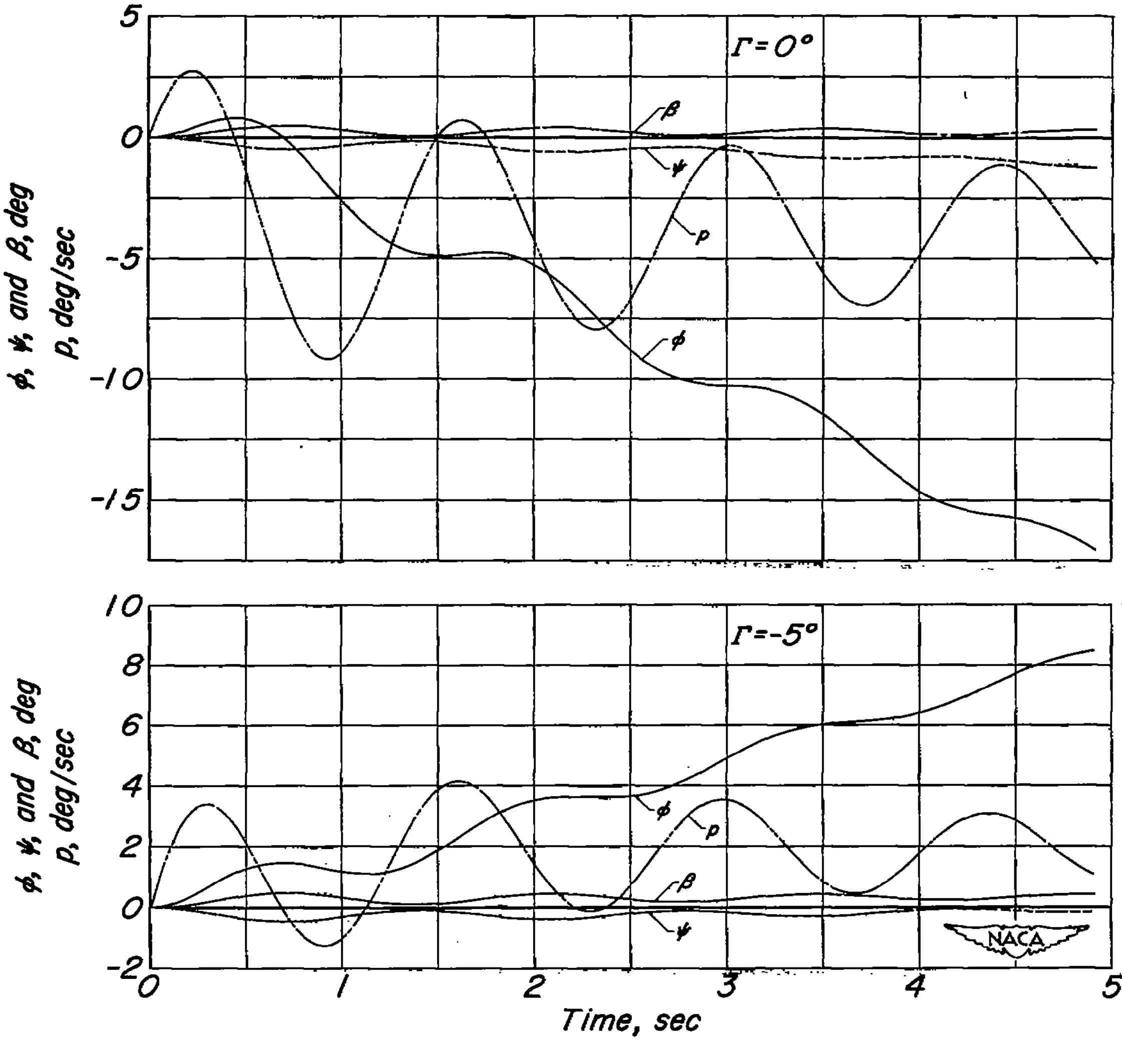

(c) Condition VII, M = 2.0 at 35,000 feet.

Figure 6.- Concluded.

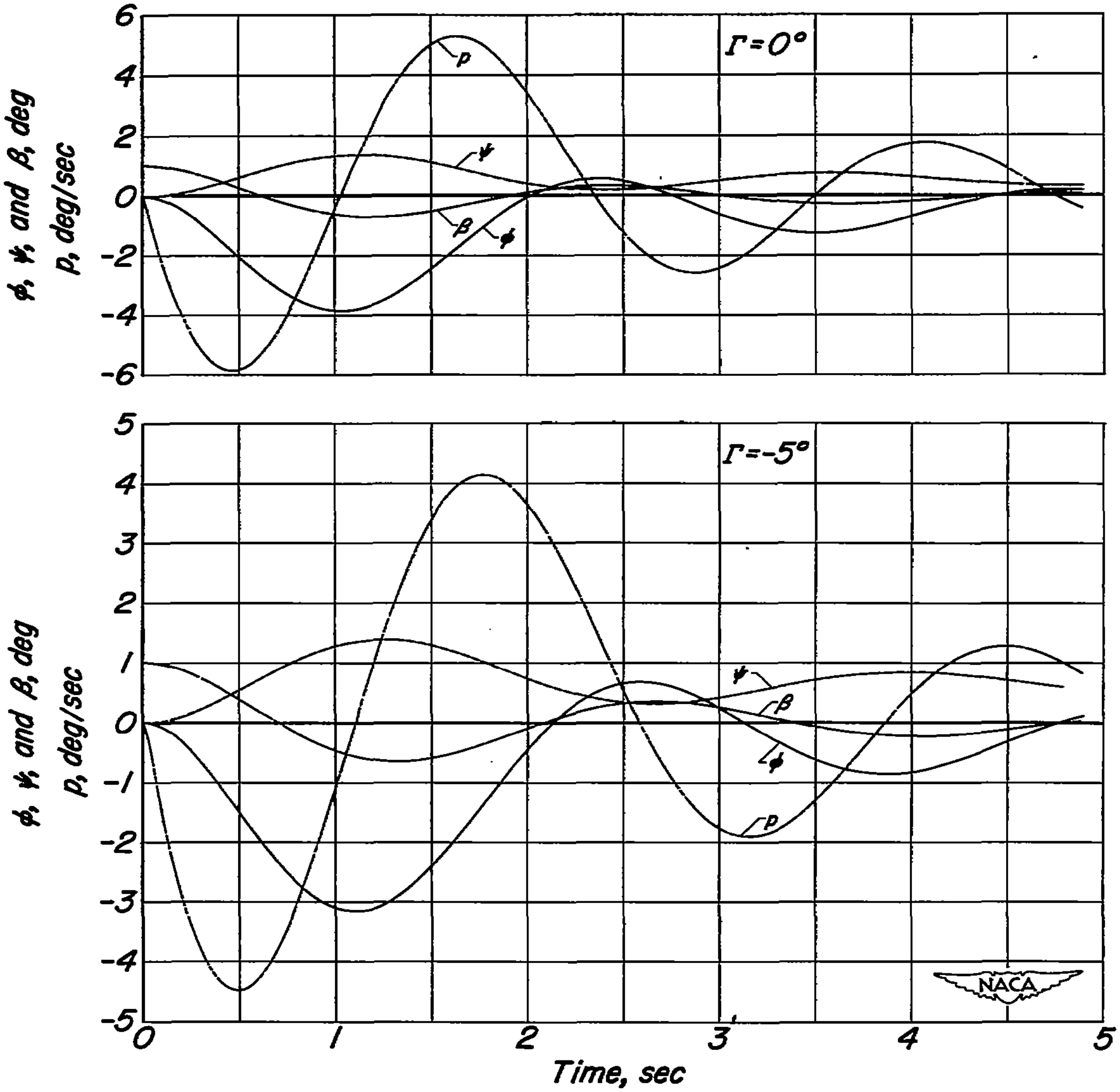

(a) Condition I, M = 0.30 at sea level.

Figure 7.- Lateral motion due to 1° initial sideslip.

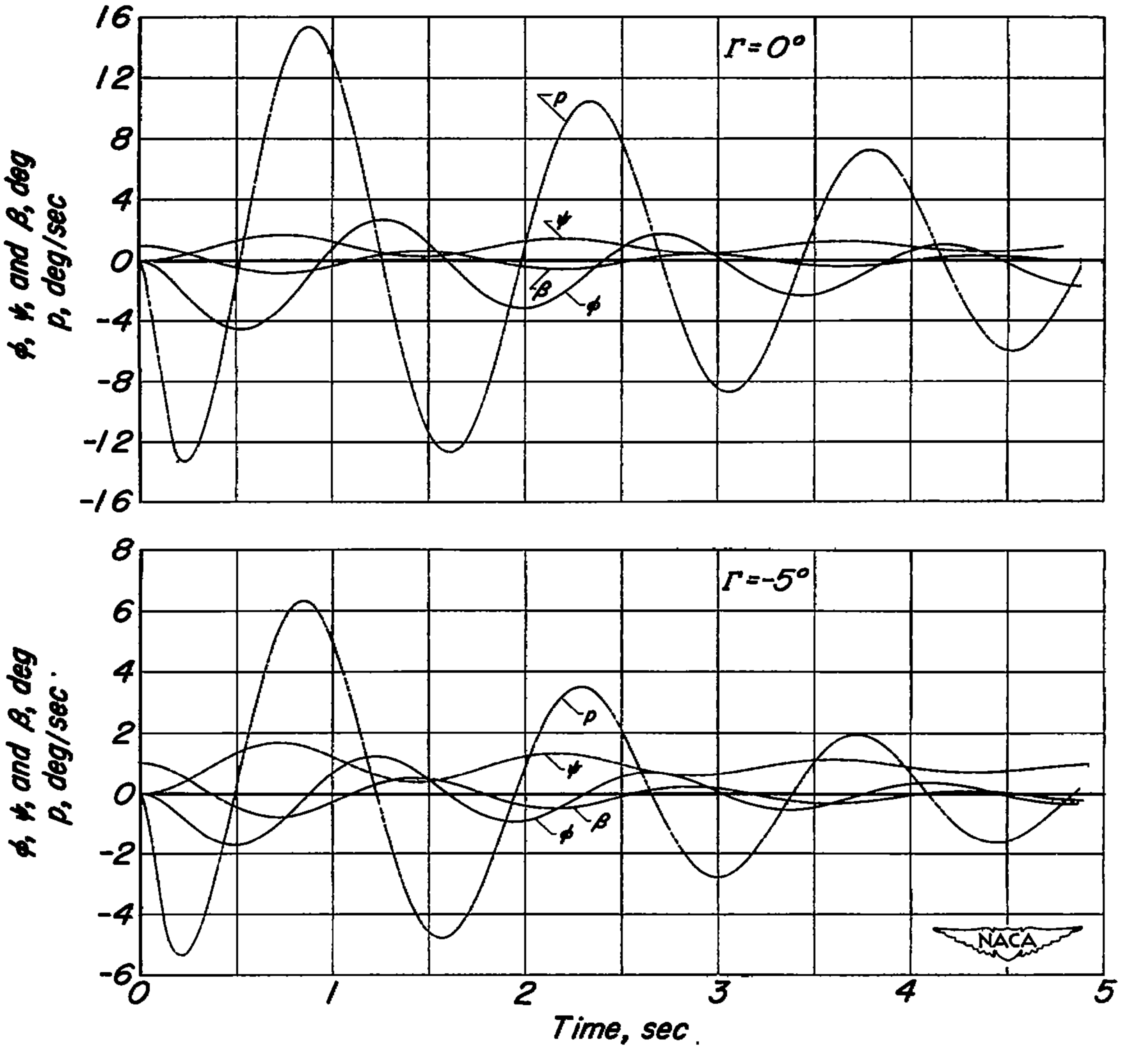

(b) Condition II, M = 0.85 at sea level.

Figure 7.- Continued.

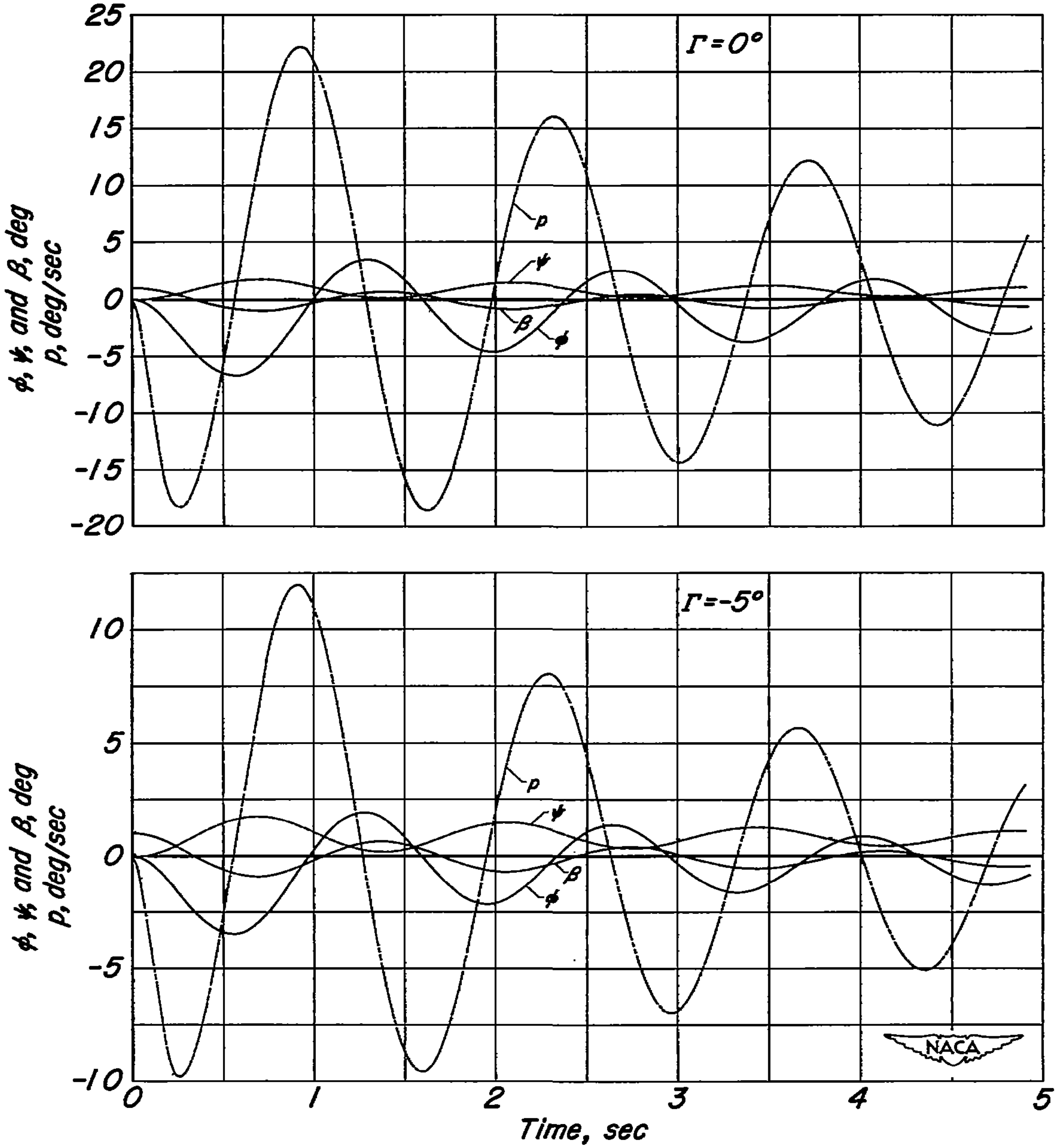

(c) Condition VII, M = 2.0 at 35000 feet.

Figure 7.– Concluded.

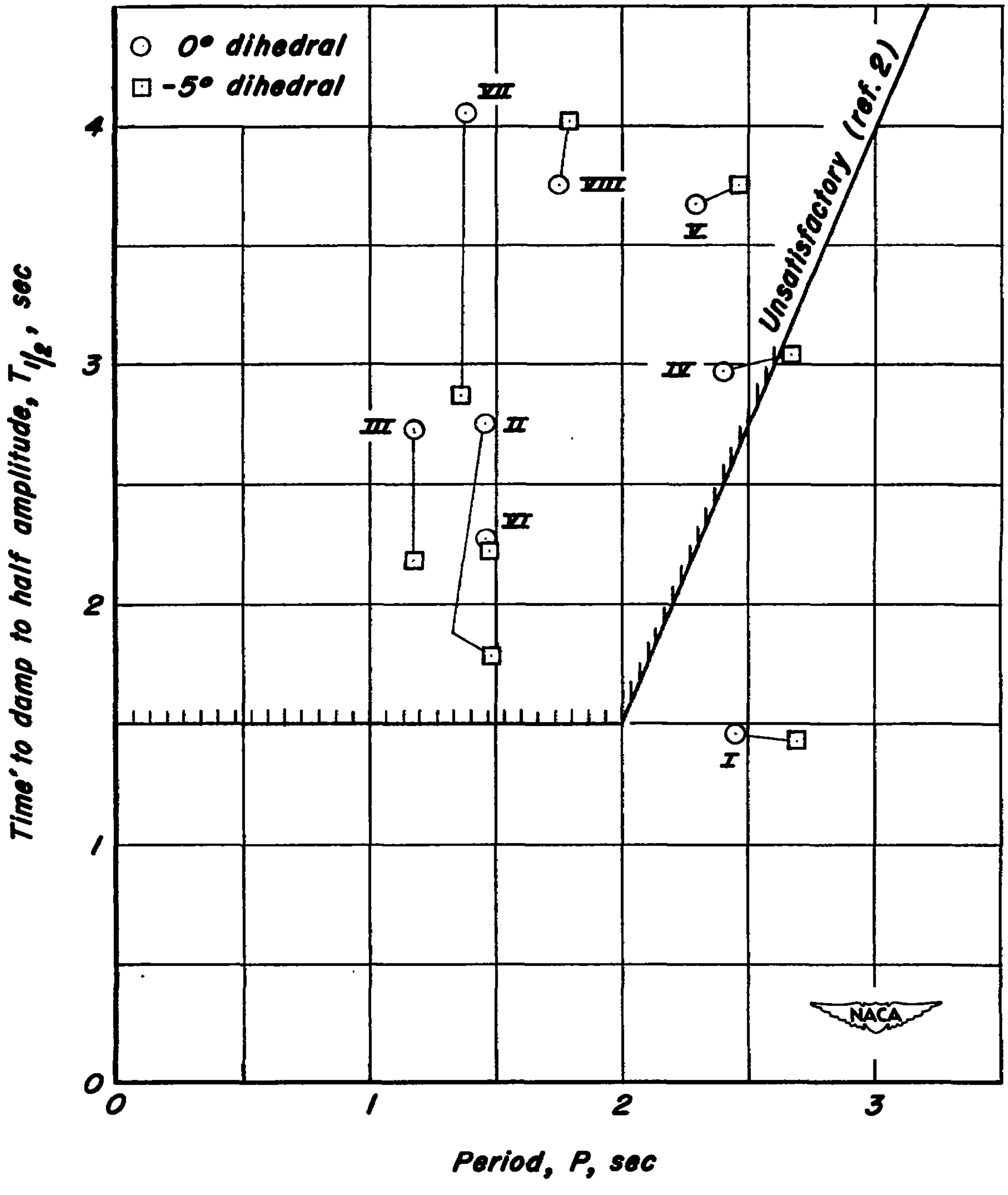

(a) Revised C_{n_p}.

Figure 8.- Period-damping relationship of the airplane with 0° and -5° geometric dihedral.

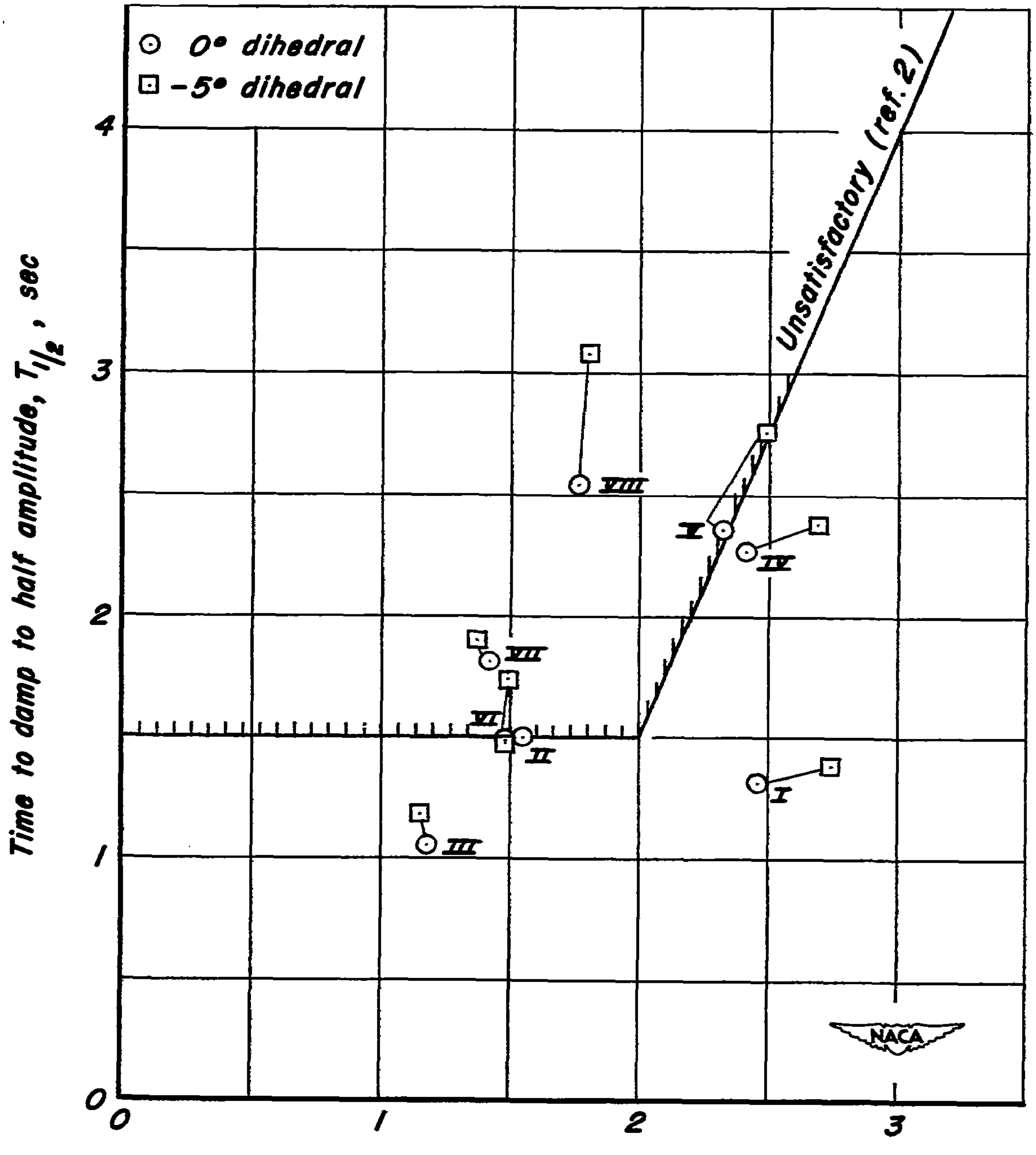

(b) Estimated C_{n_p}.

Figure 8.– Concluded.

NACA - Langley Field, Va.